Biosensors and Bioelectronics 26 (2010) 1656–1661

Contents lists available at ScienceDirect

Biosensors and Bioelectronics

journal homepage: www.elsevier.com/locate/bios

Surface plasmon resonance biosensor for parallelized detection of protein biomarkers in diluted blood plasma

Marek Piliarik, Markéta Bocková, Jiří Homola*

Institute of Photonics and Electronics AS CR v.v.i., Chaberská 57, CZ-18251 Prague 8, Czech Republic

ARTICLE INFO

Article history:
Received 17 May 2010
Received in revised form 2 August 2010
Accepted 20 August 2010

Keywords:
Surface plasmon resonance
Protein array
Cancer marker
Medical diagnostics

ABSTRACT

Surface plasmon resonance (SPR) biosensor for high-throughput screening of protein biomarkers in diluted blood plasma is reported. The biosensor combines a high-resolution SPR imaging sensor and a high-density protein array with low-fouling background. The SPR imaging sensor utilizes polarization contrast and advanced referencing and provides a total of 120 sensing areas (each 200 μm × 150 μm). Antibodies are immobilized on the sensing areas via hybridization of antibody–oligonucleotide conjugates to thiolated complementary oligonucleotides microspotted on the sensor surface (DNA-directed immobilization). A low-fouling background is achieved by covalent immobilization of bovine serum albumin to carboxyl-terminated thiols filling the areas among the thiolated oligonucleotides and outside the sensing areas. The biosensor was evaluated for detection of protein biomarkers relevant to cancer diagnostics—human chorionic gonadotropin (hCG) and activated leukocyte cell adhesion molecule (ALCAM) both in buffer and in 10% blood plasma. Limits of detection as low as 45 ng/mL (ALCAM) and 100 ng/mL (hCG) were achieved in blood plasma samples.

1. Introduction

Optical biosensors based on surface plasmon resonance (SPR) represent an established and powerful technology for investigation of biomolecular interactions. They have also been demonstrated to hold vast potential for rapid and sensitive detection of chemical and biological substances in numerous important fields such as food safety, environmental monitoring, drug development, and medical diagnostics (Homola, 2008). One of the main challenges for bioanalytical applications of SPR biosensors is achieving high sensitivity in complex real-world samples. The interferences from complex samples can influence the biomolecular interactions (Ramakrishnan et al., 2009), interfere with their observation (Baneres-Roquet et al., 2009; Kikuchi et al., 2005), and compromise specificity and detection limits of SPR biosensors (Vaisocherová et al., 2008).

Protein disease biomarkers can be found in bodily fluids such as blood plasma, saliva, and urine (Faca et al., 2008). They are present at concentrations ranging typically from pg/mL to μg/mL. For example, levels of human chorionic gonadotropin (hCG) and activated leukocyte cell adhesion molecule (ALCAM) in blood plasma of healthy individuals are around 1 ng/mL (Wu et al., 2007) and 100 ng/mL (Faca et al., 2008), respectively and can grow up to μg/mL in patients suffering from trophoblastic cancer, epithelial ovarian tumors or breast cancer (Wu et al., 2007).

Future medical diagnostic technologies are expected to detect a whole panel of protein biomarkers rather than a single biomarker (Choolani et al., 2009; Feng et al., 2009). Therefore, high-throughput biosensors capable of monitoring a large number of different binding events in parallel present a very attractive tool for biomarker screening and point-of-care diagnostics (Brennan et al., 2009; Fu et al., 2007). The most common approach to high-throughput SPR sensing is SPR imaging (Fu et al., 2007; Rich and Myszka, 2007). Common SPR imaging platforms allow for parallel monitoring of several hundreds of biomolecular interactions in the array format (Ray et al., 2010). However, fabrication of antibody arrays poses numerous challenges (Ray et al., 2010). While functionalization of sensor surface with different antibodies in conventional SPR biosensors is commonly achieved by microfluidic addressing, microfluidic structures for direct functionalization of sensor arrays are rather delicate and complex (Natarajan et al., 2008). Therefore alternative methods for fabrication of antibody microarrays have been proposed, including non-contact printing (Khan et al., 2010), micro-contact printing (Kaufmann and Ravoo, 2010), and microarraying (Lausted et al., 2008). In conjunction with antibody or peptide microarrays, SPR imaging sensors have been demonstrated to be capable of quantitative parallelized kinetic analysis of interactions of blood serum proteins (Lausted et al., 2008) and real time monitoring of auto-antibodies in 2% sera samples of autoimmune disease patients (Lokate et al., 2007). In addition, biosensors based on SPR imaging have been shown to be able to detect immunoglobulin at μg/mL levels in blood serum (Dong et al., 2008) and cancer biomarkers candidates ALCAM, and transgelin-2 at μg/mL levels

* Corresponding author. Tel.: +420 266 773 448; fax: +420 284 680 222.
E-mail address: homola@ufe.cz (J. Homola).

0956-5663/$ – see front matter © 2010 Elsevier B.V. All rights reserved.
doi:10.1016/j.bios.2010.08.063

in diluted blood serum (Ladd et al., 2009). Another challenge for SPR biosensors for bioanalysis of complex samples is associated with the nonspecific adsorption of non-target molecules on the sensing surface. Various low-fouling surfaces have been employed in (low-throughput) SPR biosensors to suppress this effect. The best low-fouling surfaces provide nonspecific adsorption in blood plasma in the order of ng/cm^2 (Vaisocherová et al., 2008). In SPR microarrays, various blocking agents (e.g. BSA, milk, gelatin) have also been used to enable detection in highly diluted blood serum samples (Lausted et al., 2008).

We report an SPR sensor for high-throughput screening of protein biomarkers in diluted blood plasma samples. The presented approach combines a recently developed high-resolution SPR imaging sensor (Piliarik et al., 2009) and a high-density protein array with a low-fouling background. Model analytes related to cancer diagnostics – ALCAM and hCG – are detected.

2. Materials and methods

2.1. Surface plasmon resonance imaging sensor

A self-referencing SPR imaging sensor with polarization contrast was recently developed at the Institute of Photonics and Electronics (Piliarik et al., 2009). This sensor is based on the Kretschmann geometry of the attenuated total reflection method and prism coupling of light into a surface plasmon (Raether, 1988). In this configuration, the spatial distribution of intensity and polarization changes of the reflected light are measured and correlated with the spatial distribution of refractive index changes on the sensor surface. A narrowband light emitted by a superluminescent diode (wavelength – 750 nm) is collimated and passed through a polarizer, a quarter-wave plate and made incident on the base of the coupling prism as depicted in Fig. 1. Light reflected from the gold layer on the SPR chip passes through the coupling prism and another polarizer. Telecentric imaging optics with 2× magnification (Edmund optics GmbH, Germany) is used to image a portion of the sensor surface (3 mm × 3 mm) on a tilted CCD camera (sca780-54fm, Basler AG, Germany). Two gold mirrors are prepared on the prism surface and the SPR chip is attached directly to this surface via a refractive index matching fluid. Light blocked and reflected by these mirrors provides reference signals enabling real time compensation for fluctuations of the dark current and intensity of incident light, respectively. The two polarizers and the quarter-wave plate are set to extinguish the reflected light corresponding to a refractive index which is slightly lower than that of the used running buffer (Piliarik and Homola, 2008). For liquid samples of near refractive indices, a change in refractive index at the surface of the sensor results in a change in the polarization of reflected light and consequently in an increase in the intensity of transmitted light. An acrylic flow-cell with gaskets made of 60 μm-thick self-adhesive vinyl foil is pressed against the SPR chip to contain a liquid sample during the experiment. The gasket forms five flow chambers on the sensor surface. Each flow chamber is 0.5 mm wide. A multichannel peristaltic pump is used to deliver five different samples simultaneously into the flow-cell. SPR chips were produced by coating SF-14 glass substrates with an adhesion-promoting titanium film (1 nm thickness) and a gold film (49 nm) by electron beam evaporation. SPR chips were washed with absolute ethanol, dried with nitrogen and cleaned in UV ozone cleaner for 10 min to remove organic contamination. After UV cleaning, the surface was washed with absolute ethanol and deionized water and blown dry with a stream of nitrogen.

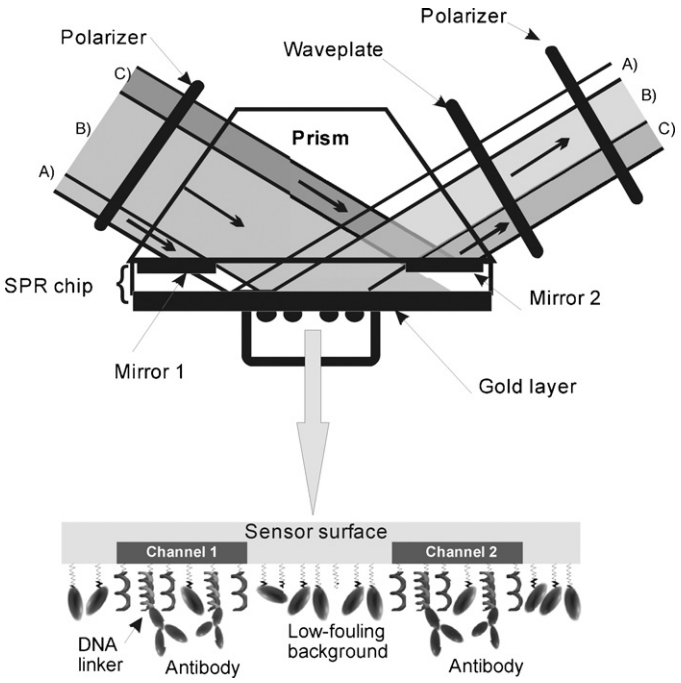

Fig. 1. Layout of the SPR imaging sensor with polarization contrast and internal referencing. The light path is divided into reference beams A) and C) and the image of the sensor surface B). Detail of the sensor surface depicts the functionalization with a protein array and a low-fouling background.

The area of the SPR chip within each flow chamber was organized into a row of sensing and reference channels. In SPR measurements, the intensity signal corresponding to each sensing or reference area was binned and normalized with the reference signals.

2.2. Sensor array

Array of antibodies was created on the sensing surface using the DNA-directed immobilization method (Ladd et al., 2004). In this method, oligonucleotides conjugated with antibodies hybridize with an array of thiolated complementary oligonucleotides microspotted on the sensor surface.

In this work, a commercial microarrayer OmniGrid (Genomic Solutions, USA) and Stealth pins (946MP4B, TeleChem International, Inc., USA) with the tip dimensions of 150 μm × 150 μm and an uptake channel for large array printing were used for the microspotting of thiolated oligonucleotides on the sensor surface. Dimensions of sensing and reference areas were 200 μm × 150 μm (two, partly overlapping spots per channel were used). Reproducibility of the position and geometry of the microarray with respect to the sensor microfluidic was in the order of 0.01 mm. Fig. 2 shows an SPR image of a sample sensor array comprising a total of 120 areas microspotted with a model protein (bovine serum albumin) for visualization. The density of the array depicted in Fig. 2 is 1500 spots/cm^2. In this study sensor arrays with the density between 1500 spots/cm^2 and 2000 spots/cm^2 were used.

The sensor array was arranged on the sensor surface to form pairs of sensing and reference areas. The distance between a sensing area and the corresponding reference area was 100 μm. This geometry was used to enable more accurate referencing of non-specific effects from complex sample. Positions of the sensing and reference channels were mapped to the image of the sensor array using a software routine developed at the Institute of Photonics and Electronics.

2.3. Calibration to refractive index change

In order to enable comparison of different experiments, the sensor response was calibrated to bulk refractive index changes. For

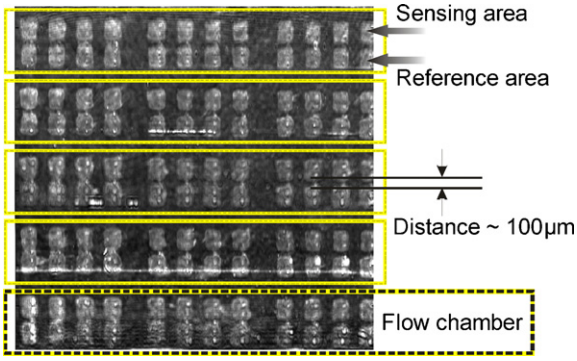

Fig. 2. Array of sensing and reference channels in the SPR image distributed in five flow chambers of the sensor. The imaged area is 3 mm × 3 mm.

that purpose, a calibration buffer was prepared by dissolving NaCl at a concentration of 0.3% in the running buffer and the corresponding refractive index change was calibrated with a commercial refractometer DSR-lambda (Schmidt Haensch GmbH, Germany). The addition of 0.3% NaCl increased the refractive index of the running buffer by 4.68×10^{-5} refractive index units (RIU). The calibration buffer was pumped for 5 min through the flow-cell. The corresponding change of sensor response was used to establish a calibration factor for each channel of the array. In the reported experiments, the sensor response is expressed in the equivalent of refractive index change expressed in 10^{-3} RIU (mRIU). It is possible to estimate the surface concentration of biomolecules on the sensor surface based on the equivalent change of refractive index (Piliarik et al., 2007). For the used SPR instrument, the surface concentration of proteins of 1 ng/cm^2 corresponds to the equivalent refractive index change of about 0.01 mRIU.

2.4. Reagents

16-Mercaptohexadecanoid acid ($HS(CH_2)_{15}COOH$) and bovine serum albumin (BSA) were purchased from Sigma–Aldrich (St. Louis, USA). Sulfo-SMPB (sulfosuccinimidyl 4-[p-maleimidophenyl]butyrate) and immobilized TCEP (Tris[2-carboxyethyl] phosphine hydrochloride) disulfide reducing gel were purchased from Pierce (Rockford, USA). Thiolated DNA probes E441C-SH (5′-/5ThioMC6-D/GGA AGG GAG TAA AGT TAA TA-3′), Sau1463-SH (5′-/5ThioMC6-D/CCT AAA AGG TTA CTC CAC CGG CT-3′) and Sau1463LC-SH (5′-/5ThioMC6-D/AGC CGGTGG AGTAACCTTTTA GG-3′) were purchased from Integrated DNA Technologies (Coralville, USA). Ethanolamine hydrochloride (EA), N-hydroxysuccinimide (NHS) and 1-ethyl-3-(3-dimethylaminopropyl) carbodiimide hydrochloride (EDC) were purchased from Biacore (Uppsala, Sweden). Human chorionic gonadotropin (hCG) and monoclonal antibody to hCG, β-subunit (anti-hCG) were purchased from Scripps Laboratories (San Diego, USA). Recombinant human ALCAM/Fc chimera (ALCAM) and monoclonal anti-human ALCAM antibody (anti-ALCAM) were purchased from R&D Systems (Minneapolis, USA). Blood plasma samples were kindly provided by the Institute of Hematology and Blood Transfusion, Czech Republic. Plasma was centrifuged from ACD whole blood of healthy donors and stored at −80 °C until use. One plasma mixture was used through all experiments reported herein; repeated freeze/thaw cycles were avoided. All other chemicals used were of analytical reagent grade.

2.5. Preparation of antibody–DNA conjugate

Antibody–DNA conjugates were synthesized as previously described (Ladd et al., 2004). Briefly, antibody (anti-hCG or anti-ALCAM) at a concentration of 0.5 mg/mL was reacted with a 10-fold molar excess of the heterobifunctional cross-linker sulfo-SMPB in PBS (100 mM phosphate, 150 mM NaCl, pH 7.4) for 30 min at a room temperature. Unreacted cross-linker was removed from the reaction solution using 30 kDa molecular weight cutoff microconcentrator (Millipore, Bedford, USA). The sample was rinsed twice with PBS and reconstituted in PBS with 5 mM EDTA (PBE). Thiolated DNA probe Sau1463LC-SH was reacted with TCEP reducing gel for 1 h and then the reducing gel was separated by centrifugation. Reduced DNA was then added to the antibody solution in 1:1 ratio and reacted for 30 min at a room temperature. Unreacted DNA was removed from the reaction solution using a 100 kDa molecular weight cutoff microconcentrator. The sample was rinsed twice with PBE and reconstituted in PBE. Product concentrations were measured using a UV spectrophotometer at wavelengths of 260 nm and 280 nm.

3. Experimental

3.1. Sensor functionalization

In order to create an antibody array with a low nonspecific response, we combined the DNA-directed immobilization (Ladd et al., 2009) and surface blocking by covalently immobilized BSA (Teramura and Iwata, 2007). This combination makes it possible to block the surface prior to the immobilization of antibody and thus avoid negative effects of surface blocking procedure on the activity of the antibody.

An array of sensing areas was prepared on the sensor surface by means of microspotting the solution of thiolated DNA probes in PBS buffer (10 mM phosphate, 2.9 mM KCl, 137 mM NaCl, pH 7.4). We investigated the effect of concentration of DNA probes on the hybridization efficiency for concentrations of probes from 5 μM to 20 μM and found that the hybridization efficiency varies by less than 5% for concentrations between 10 μM and 20 μM. Both these concentrations were used in this work and arrays utilized in this paper were fabricated using solution of 10 μM SAU1436-SH (sensing areas) and 20 μM E441C-SH (reference areas). The microspotting took place in a humidity chamber with 90% humidity and after the spotting procedure, the DNA spots were left to incubate in the chamber for additional 40 min before the chips were taken out. Then, the chips were dried with a stream of nitrogen and loaded in the SPR imaging sensor.

In order to provide the sensor with a low-fouling background, the microspotted surface was treated with a solution of carboxyl-terminated alkanethiols and then BSA was anchored to alkanethiols attached to the sensor surface. We optimized the procedure for the immobilization of BSA in terms of BSA concentration and length of the alkanethiols to maximize the sensor response to target proteins. All experiments were performed at a temperature of 25 °C. Tris running buffer (TE, 10 mM Tris, 150 mM NaCl, 5 mM EDTA, pH 7.4) was flowed through the flow-cell until a stable baseline was established. Solution of $HS(CH_2)_{15}COOH$ in TE at the concentration of 500 μM was flowed across the sensor surface for 40 min at a flow rate of 5 μL/min. All the following steps of the functionalization were performed at a flow rate of 15 μL/min. The sensing surface was flushed with TE running buffer and then the activation of carboxylic terminal groups was performed by injecting a (1:1) mixture of NHS and EDC for 5 min. Subsequently, TE buffer was injected again and switched to the modified Tris buffer TE6 (10 mM Tris, 150 mM NaCl, 5 mM EDTA, pH 5.9). The TE6 solution with BSA (1.5 mg/mL) was flowed along the activated surface for 5 min and TE6 was then injected again. In order to remove the non-covalently bound BSA, the sensor surface was treated with the high ionic strength PBNa buffer (10 mM phosphate, 0.75 M NaCl, pH 7.4, 5 min).

Antibody–DNA conjugates were immobilized on the sensor surface. First, TE buffer was flowed along the surface until a stable baseline was achieved. Then, the antibody–DNA conjugates (20× diluted in TE) were flowed for 5 min through the flow-cell and immobilized on the sensor surface via DNA hybridization with SAU1436-SH probes microspotted in the sensing areas. The immobilization of antibodies was monitored in real time with the SPR imaging sensor to assess the level of immobilized antibody. Areas of sensing surface corresponding to reference channels (microspotted with E441C-SH probes) were found to exhibit no measurable response to the immobilization of antibodies. After a short washing in TE buffer, residual carboxylic groups were deactivated with EA (1 M, pH 8.5) pumped through the flow-cell for 5 min. Finally, the sensor surface was flushed with diluted 10% blood plasma for 10 min.

3.2. Detection of protein biomarkers

SPR imaging sensor functionalized with the protein array was used to detect model protein biomarkers – hCG and ALCAM – in buffer and 10% blood plasma. All detection experiments were carried out with TENa running buffer (10 mM Tris, 0.75 M NaCl, 5 mM EDTA, pH 7.4) and a flow rate of 20 μL/min. This flow rate corresponds to a rather high flow velocity in the chamber (10 mm/s) and was found to lead to more reproducible detection experiments than lower flow rates (flow velocities). Different concentrations of protein biomarkers were diluted in 10% blood plasma, or in the TENa running buffer. Human blood plasma samples were diluted in TE buffer containing 1% BSA. The addition of BSA molecules to blood plasma samples was found to reduce the nonspecific interaction of plasma proteins with the sensing surface. After establishing a stable baseline in TENa running buffer, different samples containing hCG or ALCAM at concentrations between 10 ng/mL and 1000 ng/mL spiked in blood plasma or TENa buffer were flowed through different chambers of the flow-cell for 10 min. A corresponding "blank sample" of diluted blood plasma or TENa buffer was flowed through one of the flow chambers in each detection experiment. Finally, TENa running buffer was introduced to determine the level of bound analyte. Desorption of analyte was monitored until a stable baseline was reached. As the sensor response to analyte is directly proportional to the concentration of immobilized antibodies, the sensor response was corrected for unequal amounts of antibodies immobilized in different sensing channels.

4. Results and discussion

4.1. Performance characteristics of the SPR imaging sensor

Performance of the SPR imaging sensor was evaluated in terms of baseline noise, channels uniformity, and correlation between sensing and reference channels. The standard deviation of baseline noise calculated in all 120 channels of the sensor array was 4×10^{-7} RIU and the variation of the standard deviation for different channels was less than 20%. Sensor response obtained from a pair of sensing and reference channels was found to be correlated with a Pearson correlation coefficient of 0.5. Reference-compensated sensor response was determined by subtracting the sensor response in the reference channel from that in the adjacent sensing channel. The average baseline noise of the reference-compensated sensor response was 3×10^{-7} RIU. This result indicates that a part of the sensor response variation is associated with mechanical instabilities or flow inhomogeneities within the microfluidic channel. As these inhomogeneities affect the sensing and reference channels in the same fashion, the use of adjacent reference channels improves noise and uniformity of the sensor response across the sensor array.

4.2. Blood plasma matrix effect

To investigate the effect of blood plasma on the sensor surface, a 10% human blood plasma diluted in TE buffer containing 1% BSA was pumped through the flow chamber for 10 min; then it was replaced with the TENa running buffer. The sensor response was measured in all sensing and reference channels and the level of nonspecific adsorption was estimated from the difference of the sensor response prior to the plasma injection and 2 min after return to the running buffer. The average sensor response to nonspecific binding calculated from all 120 channels was 0.052 mRIU, which corresponds to approximately 5 ng/cm^2 of adsorbed protein. The standard deviation of the difference between the corresponding sensing and reference channels was 0.004 mRIU. Fig. 3 presents the amount of nonspecifically adsorbed blood plasma in sensing and reference channels within a single flow chamber. Clearly, the nonspecific adsorption from the blood plasma sample is not uniform across the imaged area of the flow chamber (0.5 mm × 3 mm) and decreases along the flow channel as much as by 30%. The non-uniformity of the sensor response can be attributed to the depletion of the plasma proteins in the vicinity of the sensor surface and to the non-uniform response of the sensor array itself. The difference of the sensor response of the sensing and reference channels falls within 1 ng/cm^2.

4.3. Detection of model protein biomarkers

The SPR imaging sensor was combined with the protein array of anti-ALCAM and anti-hCG antibodies and the respective proteins were detected. The surface concentrations of the immobilized antibodies in all the sensing channels were calculated from the sensor response to the immobilization of antibody–DNA conjugates. Surface concentrations of anti-ALCAM and anti-hCG were found to be 44 ng/cm^2 and 46 ng/cm^2, respectively. This corresponds to approximately 13 pg of antibody on each sensing spot. The channel-to-channel variability of the amount of the immobilization antibody, expressed as a standard deviation, was around 10%.

The detection of hCG and ALCAM biomarkers was carried out both in the TENa running buffer and diluted 10% blood plasma. The average reference-compensated response to blank plasma

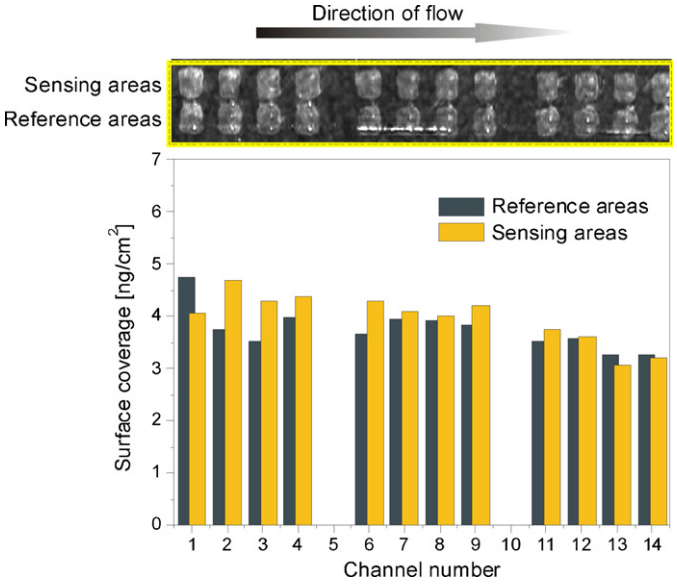

Fig. 3. Sensor response to 10% blood plasma in reference and sensing channels as a function of the position of the channel along a single flow chamber.

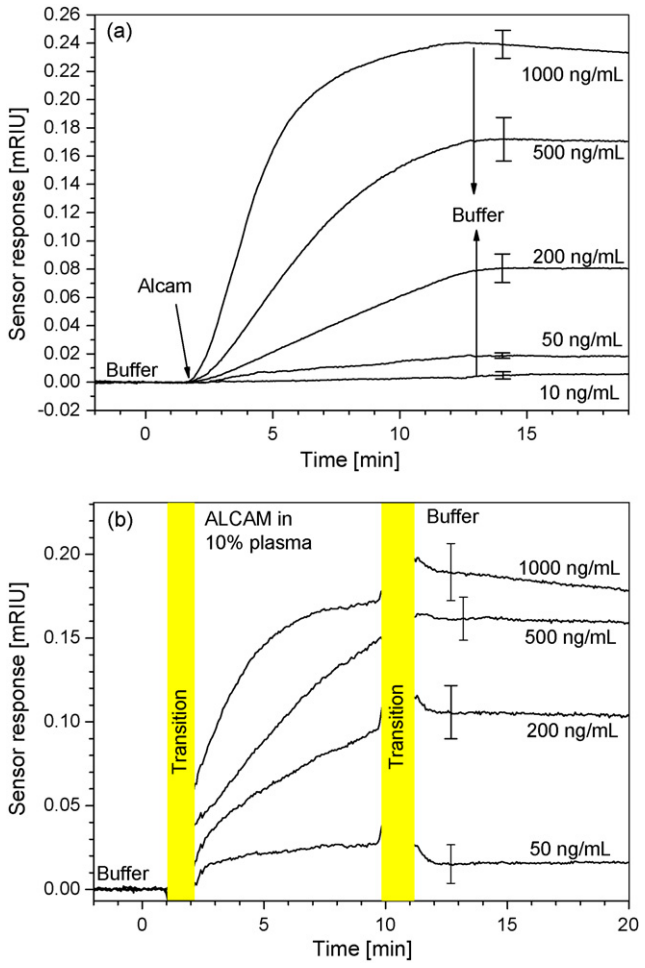

Fig. 4. Temporal sensor response to different concentrations of ALCAM protein biomarker in (a) TENa buffer and (b) 10% blood plasma. Averaged kinetics are shown and error bars indicate ±standard deviation. Vertical bars indicate the time interval required for exchanging the running buffer and blood plasma sample.

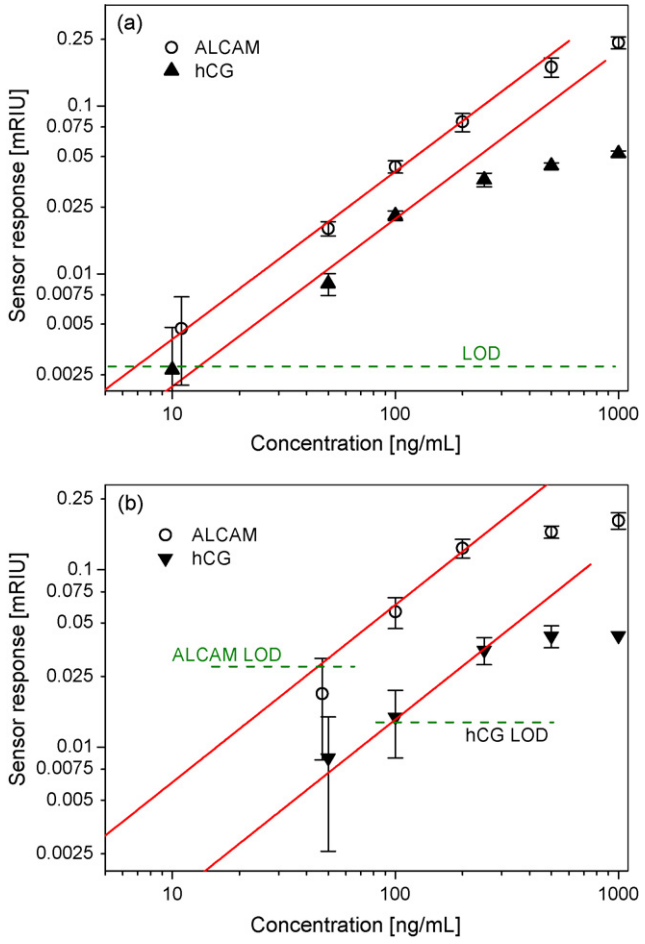

Fig. 5. Calibration curve. Detection of ALCAM and hCG in (a) TENa buffer and (b) diluted blood plasma. Straight lines in the plot represent a linear fit through zero of the linear part of each calibration curve. Dashed lines indicate the level of sensor response corresponding to LOD.

sample (without ALCAM and hCG) was 0.029 ± 0.006 mRIU and 0.03 ± 0.01 mRIU for anti-hCG array and anti-ALCAM array, respectively. The value of reproducibility of the nonspecific sensor response suggests that it is possible to resolve specific binding of protein analytes of less than 0.01 mRIU (corresponds to the surface coverage of 1 ng/cm^2). Reference measurements carried out in running buffer showed no measurable sensor response to the blank sample.

Fig. 4 compares the temporal sensor response to the binding of different concentrations of protein biomarker ALCAM in buffer (Fig. 4a) and in 10% blood plasma (Fig. 4b). Both figures show a strong concentration-dependent sensor response. The shape as well as the amplitude of the sensor response to the spiked blood plasma sample agree well with those observed when detecting ALCAM in buffer. The transition observed during the exchange of blood plasma sample and the running buffer (Fig. 4b) is associated with the replacement of a solution by another solution of substantially different composition. During this replacement, the intermixing of the two solutions occurs and the complete replacement of one solution by the other in the flow chamber takes approximately 1 min. In Fig. 4a no transition is present as the solution containing the analyte is the running buffer.

Fig. 5 compares the dependence of the reference-compensated sensor response to hCG and ALCAM on the concentration in both buffer (Fig. 5a) and blood plasma (Fig. 5b). Calibration curves show a linear dependence of the sensor response on the concentration for low protein concentrations (below 250 ng/mL for hCG and below 500 ng/mL for ALCAM). At higher protein concentrations the sensor response levels off. The sensor response to hCG was on average approximately five times lower than the response to ALCAM. This difference is believed to be associated with the hCG's lower molecular weight (approximately three times) and higher affinity of ALCAM to its antibody. The reproducibility of the sensor response for higher concentrations (above 200 ng/mL) is better than 90% when measured in buffer and better than 80% in blood plasma samples. For lower concentrations, the reproducibility decreased proportionally to the protein concentration as shown in Fig. 5. The difference between calibration curves obtained in blood plasma samples (Fig. 5b) and in buffer samples (Fig. 5a) was less than 30% for both hCG and ALCAM.

The limit of detection (LOD) was determined as a concentration which corresponds to three standard deviations of the sensor response to a blank sample. The chip-to-chip standard deviation of the sensor response to blank sample was 0.001 mRIU for both hCG and ALCAM in buffer. Using the calibration curve (Fig. 5a) these values can be translated to LOD of 7 ng/mL for ALCAM and 13 ng/mL for hCG. In blood plasma, the standard deviation of the blank sample was 0.01 mRIU and 0.006 mRIU for the detection of ALCAM and hCG, respectively. Using the calibration curve (Fig. 5b), the LODs for ALCAM and hCG were determined to be 45 ng/mL and 100 ng/mL, respectively. These LODs are higher by approximately an order of magnitude than those established in

buffer. This increase in LOD is mainly due to the nonspecific sensor response. Further improvements of the LOD can therefore be achieved by improving the fouling properties of the SPR sensing surface.

5. Conclusions

We have developed an SPR sensor for high-throughput screening of protein biomarkers in complex samples such as blood plasma. The presented approach is based on SPR imaging sensor with polarization contrast and a high refractive index resolution and a high-density antibody array produced by DNA-directed immobilization. This immobilization method allows for fabrication of protein arrays with controlled levels of immobilized antibodies and low-fouling background. The developed antibody microarrays exhibited the nonspecific protein adsorption of less than 5 ng/cm^2 for 10% human plasma which is comparable to the best low-fouling surfaces employed in conventional SPR biosensors. The sensor was demonstrated to be able to detect the binding of protein analytes in 10% blood plasma resulting in the surface coverage of less than 1 ng/cm^2. Detection of two protein biomarkers relevant to cancer diagnostics, human chorionic gonadotropin (hCG) and activated leukocyte cell adhesion molecule (ALCAM) has been demonstrated both in buffer and in blood plasma samples at clinically relevant levels. The limits of detection (LODs) for ALCAM and hCG in buffer were 7 ng/mL and 13 ng/mL, respectively. LODs for ALCAM and hCG in 10% blood plasma were determined to be 45 ng/mL and 100 ng/mL, respectively. These detection limits are comparable to those achieved with the low-throughput SPR biosensors.

Acknowledgements

This research was supported by the Academy of Sciences of the Czech Republic under the contract KAN200670701.

References

Baneres-Roquet, F., Gualtieri, M., Villain-Guillot, P., Pugniere, M., Leonetti, J.P., 2009. Antimicrob. Agents Chemother. 53 (4), 1528–1531.
Brennan, D., Justice, J., Corbett, B., McCarthy, T., Galvin, P., 2009. Anal. Bioanal. Chem. 395 (3), 621–636.
Choolani, M., Narasimhan, K., Kolla, V., Hahn, S., 2009. Expert Rev. Proteomics 6 (1), 87–101.
Dong, Y., Wilkop, T., Xu, D.K., Wang, Z.Z., Cheng, Q., 2008. Anal. Bioanal. Chem. 390 (6), 1575–1583.
Faca, V.M., Song, K.S., Wang, H., Zhang, Q., Krasnoselsky, A.L., Newcomb, L.F., Plentz, R.R., Gurumurthy, S., Redston, M.S., Pitteri, S.J., Pereira-Faca, S.R., Ireton, R.C., Katayama, H., Glukhova, V., Phanstiel, D., Brenner, D.E., Anderson, M.A., Misek, D., Scholler, N., Urban, N.D., Barnett, M.J., Edelstein, C., Goodman, G.E., Thornquist, M.D., McIntosh, M.W., DePinho, R.A., Bardeesy, N., Hanash, S.M., 2008. PLoS Med. 5 (6), 953–967.
Feng, B., Yue, F., Zheng, M.H., 2009. Adv. Clin. Chem. 47, 45–57.
Fu, E., Chinowsky, T., Nelson, K., Johnston, K., Edwards, T., Helton, K., Grow, M., Miller, J.W., Yager, P., 2007. Oral-based Diagn. 1098, 335–344.
Homola, J., 2008. Chem. Rev. 108 (2), 462–493.
Kaufmann, T., Ravoo, B.J., 2010. Polym. Chem. 1 (4), 371–387.
Khan, M.S., Fon, D., Li, X., Tian, J.F., Forsythe, J., Garnier, G., Shen, W., 2010. Colloids Surf. B: Biointerfaces 75 (2), 441–447.
Kikuchi, Y., Uno, S., Nanami, M., Yoshimura, Y., Iida, S., Fukushima, N., Tsuchiya, M., 2005. J. Biosci. Bioeng. 100 (3), 311–317.
Ladd, J., Boozer, C., Yu, Q.M., Chen, S.F., Homola, J., Jiang, S., 2004. Langmuir 20 (19), 8090–8095.
Ladd, J., Taylor, A.D., Piliarik, M., Homola, J., Jiang, S.Y., 2009. Anal. Bioanal. Chem. 393 (4), 1157–1163.
Lausted, C., Hu, Z.Y., Hood, L., 2008. Mol. Cell. Proteomics 7 (12), 2464–2474.
Lokate, A.M.C., Beusink, J.B., Besselink, G.A.J., Pruijn, G.J.M., Schasfoort, R.B.M., 2007. J. Am. Chem. Soc. 129 (45), 14013–14018.
Natarajan, S., Katsamba, P.S., Miles, A., Eckman, J., Papalia, G.A., Rich, R.L., Gale, B.K., Myszka, D.G., 2008. Anal. Biochem. 373 (1), 141–146.
Piliarik, M., Homola, J., 2008. Sens. Actuators B 134 (2), 353–355.
Piliarik, M., Párova, L., Homola, J., 2009. Biosens. Bioelectron. 24 (5), 1399–1404.
Piliarik, M., Vaisocherová, H., Homola, J., 2007. Sens. Actuators B 121 (1), 187–193.
Raether, H., 1988. Springer Tracts in Modern Physics, vol. 111, pp. 1–133.
Ramakrishnan, M., Kandimalla, K.K., Wengenack, T.M., Howell, K.G., Poduslo, J.F., 2009. Biochemistry 48 (43), 10405–10415.
Ray, S., Mehta, G., Srivastava, S., 2010. Proteomics 10 (4), 731–748.
Rich, R.L., Myszka, D.G., 2007. Anal. Biochem. 361 (1), 1–6.
Teramura, Y., Iwata, H., 2007. Anal. Biochem. 365 (2), 201–207.
Vaisocherová, H., Yang, W., Zhang, Z., Cao, Z.Q., Cheng, G., Piliarik, M., Homola, J., Jiang, S.Y., 2008. Anal. Chem. 80 (20), 7894–7901.
Wu, J., Fu, Z.F., Yan, F., Ju, H.X., 2007. TRAC-Trends Anal. Chem. 26 (7), 679–688.